Journal of sound and vibration. 2013, vol. 332, issue 4, p. 701-713. http://dx.doi.org/10.1016/j.jsv.2012.10.013

Dynamics of the electromechanical system with impact element

Marek Lampart[a,*], Jaroslav Zapoměl[b]

[a] *Department of Applied Mathematics & IT4Innovations. VŠB - Technical University of Ostrava, 17. listopadu 15/2172, 708 33 Ostrava, Czech Republic.*
[b] *Department of Mechanics. VŠB - Technical University of Ostrava, 17. listopadu 15/2172, 708 33 Ostrava, Czech Republic.*

Abstract

The main aim of the paper is to focus on the analysis of the dynamical properties of the electromechanical system with impact element. This model is constructed with three degrees of freedom in the mechanical oscillating part, two translational and one rotational. The mathematical model of the system is represented by three coupled second-order ordinary differential equations. Here, the most important nonlinearities are: stiffness of the support spring elements and internal impacts.

Keywords: electromechanical system, damping effect, nonlinear stiffness, bifurcation, impacts, irregular vibration

1. Introduction

The impacts of solid bodies are an important mechanical phenomena. Their presence can be observed during a large number of natural and technological processes. The impacts are characterized by short time lasting body collisions, very large impact forces and by almost sudden changes of system state parameters. The experience and theoretical analyses show that behavior of the impact systems is highly nonlinear, highly sensitive to initial conditions and instantaneous excitation effects frequently leading to irregular vibrations and hard to predict movements. Behavior of each system where

*Corresponding author
Email addresses: marek.lampart@vsb.cz (Marek Lampart), jaroslav.zapomel@vsb.cz (Jaroslav Zapoměl)

DSpace VŠB-TUO http://hdl.handle.net/10084/96108 2/4/2013

the body collisions take place is different and therefore, each of them must be investigated individually.

Due to the practical importance a good deal of attention is focused on analysis of vibro-impact systems where the vibrations are governed by the momentum transfer and mechanical energy dissipation through the body collisions. This is utilized at impact dampers applied to attenuate high-amplitude oscillations, such as those appearing in subharmonic, self-excited and chaotic vibrations.

Even if the problem of impacts is very old, the new possibilities of its investigation enabled by efficient computational simulations appeared at the end of the 20th century. Chaterjee at al. [1, 2] studied a dynamical behavior of an impact damper for vibration attenuation of an externally loaded and self-excited cart moving in one direction. The damping was produced by impacts of a point body colliding with the cart walls. A number of authors dealt with the so called non-ideal problem, which means that the power of the source exciting the oscillator is limited. The article of Warminski and Balthazar [3], who extended the Chaterjee's model with the cart by attaching a rotor driven by a motor, belongs to this category. Application of a non-ideal model to the gear rattling dynamics was done by de Souza et al. [4]. A new mechanical model with clearances for a gear transmission was reported by Luo and O' Connor in [5]. Their model has time varying boundaries and impacts between two gears occur at different locations. The horizontal movement of a cart excited by a rotating particle and damped by an impact damper formed by a point body bouncing on the cart walls was investigated by de Souza et al. [6]. The computational simulations confirmed the chaotic character of the oscillations. Consequently, influence of the impact body to the cart mass ratio on its suppression was examined. The non-ideal impact problem completed by flexible stops was analyzed by Zukovic and Cveticanin in [7]. The main objective was to study the character of vibration of the oscillator excited by an unbalanced rotor driven by a motor of limited power. A mutual interaction of a mechanical and electrical system was analyzed by Půst [8]. The investigated unbalanced rotor of an electric motor was attached to a cantilever beam. The amplitude of its bending vibration was limited by a flexible stop. The performed simulations were aimed at the study of the character of the induced vibration and at fluctuations of the current in the electric circuit. Vibrations of a rotor supported by bearings with nonlinear stiffness and damping characteristics considering its impacts against the stationary part were investigated by Zapoměl et al. [9]. The

DSpace VŠB-TUO http://hdl.handle.net/10084/96108 2/4/2013

Journal of sound and vibration. 2013, vol. 332, issue 4, p. 701-713. http://dx.doi.org/10.1016/j.jsv.2012.10.013

shaft was represented by a beam like-body and rotation of the disc was taken into account. The impacts were described both by collisions of rigid bodies (Newton theory) and by impacts with soft stops.

In this paper a system formed by a rotor and its casing flexibly coupled with a baseplate and of an impact body, which is separated from the casing by two, lower and upper, gaps is analyzed. The rotor is driven by a motor of limited power and from this point of view the investigated model system can be classified as non-ideal. A new contribution of the presented work consists in investigating the system oscillations as a result of a combined time variable loading caused by two sources, the rotor unbalance and the baseplate vibrations. The emphasis is put on observing the influence of the inner impacts on the character and reduction of the system vibration in dependence on the mass of the impact body. The investigated system is of great practical importance as it represents a simplified model of a rotating machine, which is excited by ground vibrations and unbalance of the rotating parts and damped by an impact damper. Results of the performed simulations contribute to better knowledge of the dynamical behavior of such technological devices and of impact systems with complicated loading, in general.

2. The vibrating system

The investigated system consists of a rotor (body 1, Figure 1), of its casing (body 2, Figure 1) and of a base plate (body 3, Figure 1), with which the rotor casing is coupled by a spring and damping element. The casing and the base plate can move in the vertical direction and the rotor can rotate and slide together with its casing. Vibration of the base plate and unbalance of the rotor are the main sources of the casing excitation. To attenuate its oscillation an impact damper has been proposed. It consists of a housing fixed to the rotor casing (body 2, Figure 1) and of an impact body (body 4, Figure 1), which is coupled with the housing by a linear spring. The impact body can move only in the vertical direction and is separated from the housing by a lower and upper clearances that limit its vibration amplitude. The rotor is loaded by an external moment produced by a DC electric motor.

The task was to investigate influence of the upper and lower clearances between the rotor casing and the impact body respectively on attenuation of the rotor frame oscillation and character of its motion.

In the computational model all bodies are considered as absolutely rigid. The spring element coupling the rotor casing and the base plate is nonlinear

DSpace VŠB-TUO http://hdl.handle.net/10084/96108 2/4/2013

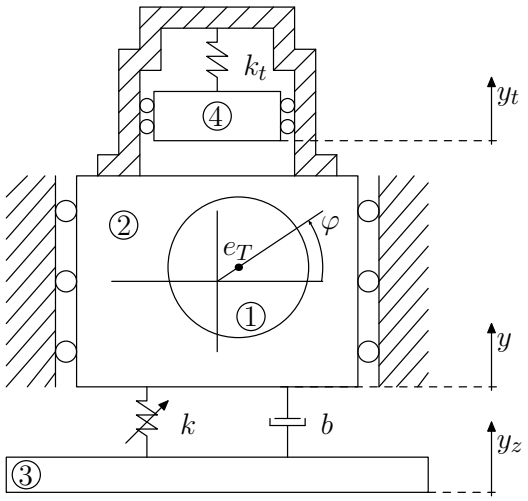

Figure 1: Model of vibrating system

showing a cubic characteristic

$$F_K = k_1\Delta + k_3\Delta^3 \tag{1}$$

where F_K is the spring force, k_1, k_3 are the stiffness parameters and Δ is the spring deformation (compression or extension). The damper and the spring coupling the impact body with the damper housing are linear. To describe the impacts the Newton theory based on validity of the momentum conservation law and the coefficient of restitution determining the mechanical energy dissipation during the impacts has been accepted.

3. Mathematical model of the system

The investigated system has 3 degrees of freedom. Its instantaneous position is defined by three generalized coordinates:

- y - vertical displacement of the rotor casing,
- y_t - vertical displacement of the impact body and
- φ - angular rotation of the rotor.

The system vibration is governed by the equations of motion that have been derived by application of the Lagrange equations of the second kind

DSpace VŠB-TUO http://hdl.handle.net/10084/96108 2/4/2013

$$\frac{\mathrm{d}}{\mathrm{d}t}\left(\frac{\partial W_K}{\partial \dot{q}_j}\right) - \frac{\partial W_K}{\partial q_j} + \frac{\partial W_P}{\partial q_j} = Q_j, \tag{2}$$

$$q_j \in \{y, y_t, \varphi\} \tag{3}$$

for $j = 1, 2, 3$. Where W_K and W_P is kinetic and potential energy of the system, respectively, q_j is the j-th generalized coordinate, Q_j is the corresponding generalized force, t is the time and $\dot{q}$ denotes the first derivative of q with respect to time.

Kinetic energy of the system is given as the sum of kinetic energies of the individual bodies

$$W_K = \frac{1}{2}m\dot{y}^2 + \frac{1}{2}m_t{\dot{y}_t}^2 + \frac{1}{2}m_R(\dot{x}_{RT}^2 + \dot{y}_{RT}^2) + \frac{1}{2}J_{RT}\dot{\varphi}^2 \tag{4}$$

where m, m_t, m_R are masses of the rotor casing, impact body and the rotor respectively, J_{RT} is the moment of inertia of the rotor relative to the axis going through its centre of mass and x_{RT}, y_{RT} are the horizontal and vertical coordinates of the rotor centre of mass.

Coordinates x_{RT}, y_{RT} can be expressed by means of generalized coordinates y and φ

$$x_{RT} = e_T\cos(\varphi), \tag{5}$$

$$y_{RT} = y + e_T\sin(\varphi). \tag{6}$$

After substitution of (5) and (6) into (4) and performing some manipulations the relation for the kinetic energy of the system has the form

$$W_K = \frac{1}{2}(m + m_R)\dot{y}^2 + \frac{1}{2}m_t{\dot{y}_t}^2 + \frac{1}{2}m_R e_T\dot{y}\dot{\varphi}\cos(\varphi) + \frac{1}{2}(J_{RT} + m_T e_T^2)\dot{\varphi}^2. \tag{7}$$

Taking into account that the spring coupling the base plate with the rotor casing has a nonlinear characteristic (1) the relation for the system potential energy accumulated in the flexible elements can be expressed

$$W_P = \frac{1}{4}k_3(y - y_z)^4 + \frac{1}{2}k_1(y - y_z)^2 + \frac{1}{2}k_t(y_t - y)^2. \tag{8}$$

Other working forces acting in the system are: the driving moment acting on the rotor, the gravitational forces and the damping force exerted by the

DSpace VŠB-TUO http://hdl.handle.net/10084/96108 2/4/2013

damper, which couples the rotor casing with the base plate. For their virtual work it holds

$$\delta A = M_M \delta\varphi - mg\delta y - b(\dot{y} - \dot{y}_t)\delta y - m_t g \delta y_t - m_R g \delta y_{RT} \tag{9}$$

where g is the gravity acceleration and M_M is the external moment, by which the motor acts on the rotor.

Utilizing relationship (6) the virtual displacements y_{RT} can be expressed

$$\delta y_{RT} = \delta y + e_T[\sin(\varphi + \delta\varphi) - \sin(\varphi)] \tag{10}$$

and consequently

$$\delta y_{RT} = \delta y + e_T \cos(\varphi)\delta\varphi. \tag{11}$$

Taking into account relation (11) the expression for the virtual work (9) can be rewritten in the form

$$\delta A = [-b(\dot{y} - \dot{y}_t) - m_R g - mg]\delta y + [-m_t g]\delta y_t + [M_M - m_R g e_T \cos(\varphi)]\delta\varphi. \tag{12}$$

The coefficients of proportionality of variations of the generalized displacements are the generalized forces

$$Q_y = -b(\dot{y} - \dot{y}_t) - m_R g - mg, \tag{13}$$

$$Q_{y_t} = -m_t g, \tag{14}$$

$$Q_\varphi = M_M - m_R g e_T \cos(\varphi). \tag{15}$$

The external moment acting on the rotor is a linear function of angular velocity of its rotation

$$M_M = M_Z - k_M \dot{\varphi} \tag{16}$$

which corresponds to a static characteristic of a DC electric motor. M_Z is the starting moment and k_M is negative of the motor characteristic slope.

Performing the derivatives of the kinetic and potential energies (7) and (8) as required by the Lagrange equation (2) and utilizing relations for the generalized forces (13) – (15) and external moment acting on the rotor gives the equations of motion of the studied system

DSpace VŠB-TUO http://hdl.handle.net/10084/96108 2/4/2013

$$\begin{aligned}(m+m_R)\ddot{y}+m_R e_T\cos(\varphi)\ddot{\varphi} &= m_R e_T\dot{\varphi}^2\sin(\varphi)-b(\dot{y}-\dot{y}_z)-\\ &\quad -k_3(y-y_z)^3-k_1(y-y_z)-\\ &\quad -k_t(y-y_t)-(m+m_R)g,\\ m_t\ddot{y}_t &= -k_t(y_t-y)-m_t g,\\ (J_{RT}+m_R e_T^2)\ddot{\varphi}+m_R e_T\cos(\varphi)\ddot{y} &= -m_R g e_T\cos(\varphi)+M_Z-k_M\dot{\varphi}\end{aligned} \tag{17}$$

where $\ddot{y}$, $\ddot{\varphi}$ denote the second derivative of y and φ respectively with respect to time.

3.1. Initial conditions

Without loss of generality it can assumed that there is no vibration in the beginning of our simulation, the system is in rest and takes the equilibrium position. Putting the speed and acceleration equal to zero we get the following initial conditions of our system.

$$\begin{aligned}\dot{y}(0) &= 0,\\ \dot{y}_t(0) &= 0,\\ \dot{\varphi}(0) &= 0,\\ k_3(y(0)-y_z(0))^3+k_1(y(0)-y_z(0))+ & \\ +k_t(y(0)-y_t(0))+(m+m_R)g &= 0,\\ k_t(y_t(0)-y(0))+m_t g &= 0,\\ \varphi(0) &= 3/2\,\pi.\end{aligned} \tag{18}$$

Let us simulate the vibration of the base plate by the map

$$y_z(t)=A\,(1-\mathrm{e}^{-\alpha t})\sin(\omega t) \tag{19}$$

where A is amplitude, α is the starting constant of y_z and ω stands for the rouse frequency, see Figure 2, so $y_z(0)=0$ and $\dot{y}_z(0)=0$.

The last two conditions of (18) could be simplified and we conclude:

Lemma 1. *Let k_1, k_3, k_t, m, m_t and m_R be real positive constants, and g be the gravity acceleration. Then there is only one real solution of the system*

$$k_3y^3(0)+k_1y(0)+k_t(y(0)-y_t(0))+(m+m_R)g = 0, \tag{20}$$

$$k_t(y_t(0)-y(0))+m_t g = 0. \tag{21}$$

DSpace VŠB-TUO http://hdl.handle.net/10084/96108 2/4/2013

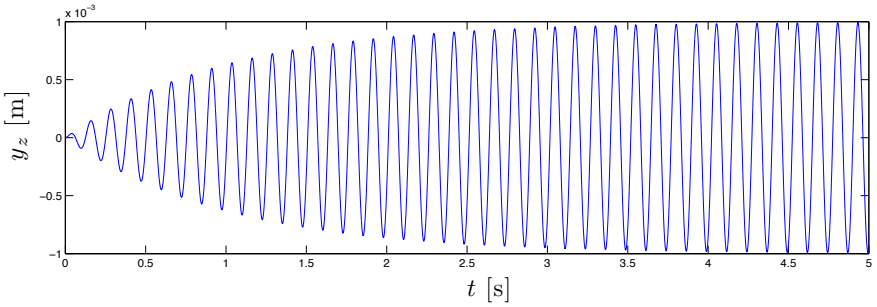

Figure 2: Vibration of the base plate given by function (19).

Moreover, the real solution equals

$$\begin{aligned} y(0) &= \sqrt[3]{-q+\sqrt{q^2+p^3}}+\sqrt[3]{-q-\sqrt{q^2+p^3}}, \\ y_t(0) &= \sqrt[3]{-q+\sqrt{q^2+p^3}}+\sqrt[3]{-q-\sqrt{q^2+p^3}}-\frac{m_t g}{k_t} \end{aligned} \tag{22}$$

where $p = k_1/3k_3$ *and* $q = ((m + m_R + m_t)g)/2k_3$.

Proof. Subtracting (21) into (20) the following is obtained

$$y^3(0) + \frac{k_1}{k_3}y(0) + \frac{(m + m_R + m_t)g}{k_3} = 0.$$

It is easy to verify that the cubic discriminant is negative of the polynomial on the left hand side, since all constants are positive. Hence, there is one real and two non-real complex conjugate roots. To the end, equations given by (22) are *Cardano's formulas*.

3.2. New initial conditions

The motion of the impact body is limited by vibration of the rotor casing. If the limit position given by the conditions

$$y - y_t = -c_1 + \delta_e, \quad \dot{y}_t > \dot{y}, \tag{23}$$

$$y - y_t = c_2 + \delta_e, \quad \dot{y}_t < \dot{y} \tag{24}$$

DSpace VŠB-TUO http://hdl.handle.net/10084/96108 2/4/2013

is reached, the impact occurs. Constants c_1 and c_2 denote the width of the upper and lower clearances between the rotor casing and the impact body respectively at the moment when the system takes the equilibrium position, and

$$\delta_e = \frac{m_t g}{k_t}$$

denotes extension of the spring element of the stiffness k_t caused by the weight of the impact body. If the impact takes place, the momentum conservation law and the condition for expressing dissipation of the mechanical energy must be satisfied

$$\begin{aligned} (m+m_R)\dot{y}_1 + m_t\dot{y}_{t1} &= (m+m_R)\dot{y}_2 + m_t\dot{y}_{t2}, & (25)\\ \dot{y}_2 - \dot{y}_{t2} &= -\varepsilon_R(\dot{y}_1 - \dot{y}_{t1}) & (26) \end{aligned}$$

where $\dot{y}_1$ and $\dot{y}_{t1}$ denote velocities of the rotor casing and the impact body before the impact, $\dot{y}_2$ and $\dot{y}_{t2}$ their velocities after the impact and ε_R is the constant of restitution, $\varepsilon_R \in (0,1)$.

From (25) and (26) new initial conditions are estimated for the system (17)

$$\begin{aligned} \dot{y}_2 &= \frac{m+m_R}{m+m_R+m_t}\left[\dot{y}_1 + \frac{m_t}{m+m_R}\dot{y}_{t1} - \frac{m_t}{m+m_R}\varepsilon_R(\dot{y}_1 - \dot{y}_{t1})\right],\\ \dot{y}_{t2} &= \frac{m+m_R}{m+m_R+m_t}\left[\dot{y}_1 + \frac{m_t}{m+m_R}\dot{y}_{t1} + \varepsilon_R(\dot{y}_1 - \dot{y}_{t1})\right]. \end{aligned} \quad (27)$$

The equations of motion (17) represent a set of nonlinear mutually coupled ordinary differential equations of the second order. Because of conditions (24) and (23), their solution is continuous (but not smooth, see Figures 4, 7 and 10) in system displacements and discontinuous in velocities (see Figures 5, 8 and 11). For their solving an implicit Adams-Moulton method has been applied. If the impact occurs, the solution is interrupted, new initial conditions (velocities of the rotor casing and impact body) are calculated by (27) and the solution proceeds with the newly determined initial conditions.

4. Main results

Figure 3 shows the dependence of the pick to pick amplitude of the rotor frame vibration on angular frequency of excitation of the base plate in case

DSpace VŠB-TUO http://hdl.handle.net/10084/96108 2/4/2013

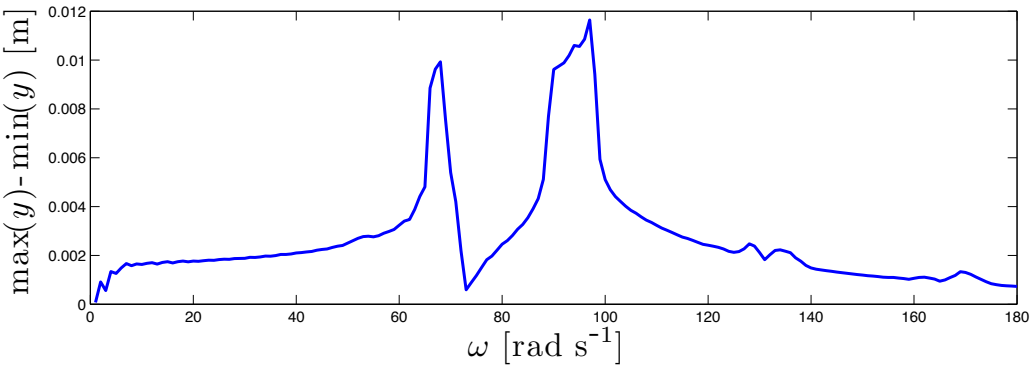

Figure 3: The dependence of the pick to pick amplitude of the rotor frame vibration on angular frequency of excitation of the base plate for unlimited movement of the impact body, for $m_t = 15$ kg.

that the movement of the impact body is not limited (clearances are sufficiently large, $m_t = 15$ kg), two resonance picks are observed here. Based on this result the following numerical simulations were performed for the system parameters summarized in Table 1 and for the source frequency of 97 rad s^{-1} which corresponds to the second resonance pick.

Next, the parameters c_1 and c_2 are taken as variable. There are three situations discussed in detail depending on the upper and lower clearances between the rotor casing and the impact element respectively. They were determined to be equal for simplicity.

For the first simulation, let be the clearance $c_1 = c_2 = 2$ mm:

- time responses of the investigated system are given in Figure 4, displacements y and y_t are harmonic in this case, there are impacts on both sides,
- velocities of the impact element $\dot{y}_t$ and the casing $\dot{y}$ are given in Figure 5,
- magnification of the graphs y_t and $\dot{y}_t$ are in Figure 6, function y_t is not smooth and $\dot{y}_t$ is not continuous since there are impacts,
- phase portrait: $y-y_t$ versus $\dot{y}-\dot{y}_t$ is in Figure 14a, double-sided impacts are observed, see Figure 15, and the attractor is almost periodic, see Figure 13a.

DSpace VŠB-TUO http://hdl.handle.net/10084/96108 2/4/2013

In this case, the total vibration of the body (the difference between maximum and minimum values of y) is equal to 3.54 mm, see Figures 15 and 16. Let us point out that $\max y_z - \min y_z = 2$ mm for given parameters, see Figure 2. Hence, there is no significant attenuation of the rotor frame oscillation for $c_1 = c_2 = 2$ mm.

Now, let us increase the clearance to $c_1 = c_2 = 8$ mm. So,

- time responses of the investigated system are given in Figure 7, there are double-sided impacts between the impact body and the rotor frame,
- velocities of the impact element $\dot{y}_t$ and the casing $\dot{y}$ are given in Figure 8,
- magnification of the graphs y_t and $\dot{y}_t$ around the impact time are in Figure 9, function y_t is not smooth and $\dot{y}_t$ is not continuous since there are impacts,
- phase portrait: $y - y_t$ versus $\dot{y} - \dot{y}_t$ is in Figure 14b, double-sided impacts are observed as well as periodic (or very close to periodic) attractor, see Figures 15 and 13b.

In this case, the total vibration of the body (the difference between maximum and minimum values of y) is equal to 1.67 mm while the total vibration of the base plate is 2 mm, see Figures 15 and 16. Hence, there is significant attenuation of the rotor frame oscillation for $c_1 = c_2 = 8$ mm.

Finally, let us do the simulation for $c_1 = c_2 = 30$ mm:

- time responses of the investigated system are given in Figure 10, there are no impacts,
- velocities of the impact element $\dot{y}_t$ and the casing $\dot{y}$ are given in Figure 11,
- magnification of graphs y_t and $\dot{y}_t$ around the impact time are in Figure 12, booth functions y_t and $\dot{y}_t$ are smooth since there are no impacts,
- phase portrait: $y - y_t$ versus $\dot{y} - \dot{y}_t$ is showing chaotic behavior, see Figures 14f, 13f and 15.

In this case, the total vibration of the body (the difference between maximum and minimum value of y) equals to 14.09 mm, see Figures 15 and 16. Hence, the vibration of the body was not reduced.

DSpace VŠB-TUO http://hdl.handle.net/10084/96108 2/4/2013

The Fourier spectra (Figure 13) and phase trajectories (Figure 14) show that the movement is formed by a number of harmonic components having the basic, super-harmonic, sub-harmonic and combination frequencies on which there are superposed further motions with frequencies forming the sided bands of dominant frequencies. Their mutual ratio indicates the irregularity of the vibration. For the clearance width up to 8 mm the vibration is periodic or almost periodic. A significant increase of the motion irregularity occurs at the clearance width of 9 mm and 16 mm when the motion can be considered as quasi-periodic and chaotic respectively. For clearances 20 – 21 mm the regularity of the motion sharply increases (the motion becomes quasi-periodic). In the intervals of 9 – 15 mm and 20 – 21 mm the phase trajectory finds itself in a close neighborhood of the carrying cycle.

The Figure 15 clearly shows the values of clearances at which the bifurcation occurs. For clearance smaller than 26 mm there are double-sided impacts. After exceeding the value of 27 mm, the system starts to perform a motion without impacts.

The damping effect of the impact body is evident form Figure 16, where simulations show the best choice of the clearance, that is 8 mm in our test.

The Figure 17 is a bifurcation diagram it shows relative displacements of the rotor frame with respect of the impact body taken with the period of the base plate excitation in dependence on the clearances. It is evident that for clearances less than 9 mm the relative motion is regular and periodic, for higher magnitudes of the clearances the motion becomes irregular having a quasi-periodic character or character with chaotic component, see Figure 13.

5. Conclusions

In the paper, a new electro mechanical model with impact element was developed and analyzed. This model was inspired by real frequently occurring technological problems when electromechanical rotating machines are excited by a combined loading produced by the rotor unbalance and ground vibrations. The equations of motion are solved numerically by the implicit Adamso-Moulton method and solutions for given parameters are reported. Dynamics of the model is forced not only by the rotor unbalance but also by vibration of the base plate that plays the key role here. The computational simulations proved that application of the impact body resulted in a significant decrease in vibration amplitude of the rotor frame.

DSpace VŠB-TUO http://hdl.handle.net/10084/96108 2/4/2013

value	quantity	format	description
m	100	kg	mass of the dumping body
m_R	40	kg	mass of the rotor
m_t	15	kg	mass of the impact element
k_1	1.5×10^5	N m^{-1}	linear stiffness coefficient
k_3	6×10^{10}	N m^{-3}	cubic stiffness coefficient
J_{RT}	5	kg m^2	moment of inertia of the rotor
b	1.5×10^3	N s m^{-1}	damping coefficient of the suspension
k		N m^{-1}	stiffness of the suspension spring
k_t	8×10^4	N m^{-1}	coupling stiffness of the impact element
e_T	2	mm	eccentricity of the rotor center of gravity
φ		rad	rotation angle of the rotor
M_Z	100	N m	starting moment
k_M	8	N m s rad^{-1}	negative of the motor characteristic slope
ε_R	0.5		restitution constant
α	1		starting constant of y_z
ω	97	rad s^{-1}	source frequency constant of y_z
A	1	mm	amplitude of y_z

Table 1: Parameters of the system (17).

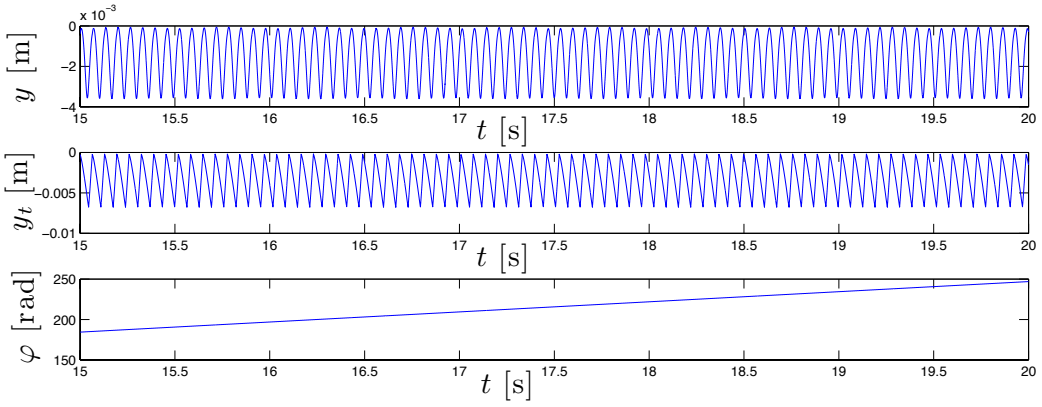

Figure 4: Time responses of the system (17) with parameters given in Table 1 for $c_1 = c_2 = 2$ mm.

DSpace VŠB-TUO http://hdl.handle.net/10084/96108 2/4/2013

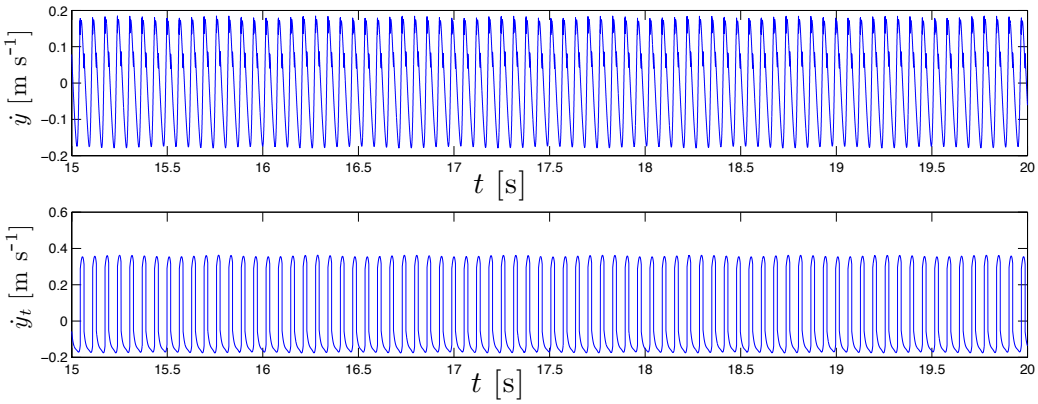

Figure 5: Velocities of an impact element $\dot{y}_t$ and a casing $\dot{y}$ of the system (17) with parameters given in Table 1 for $c_1 = c_2 = 2$ mm.

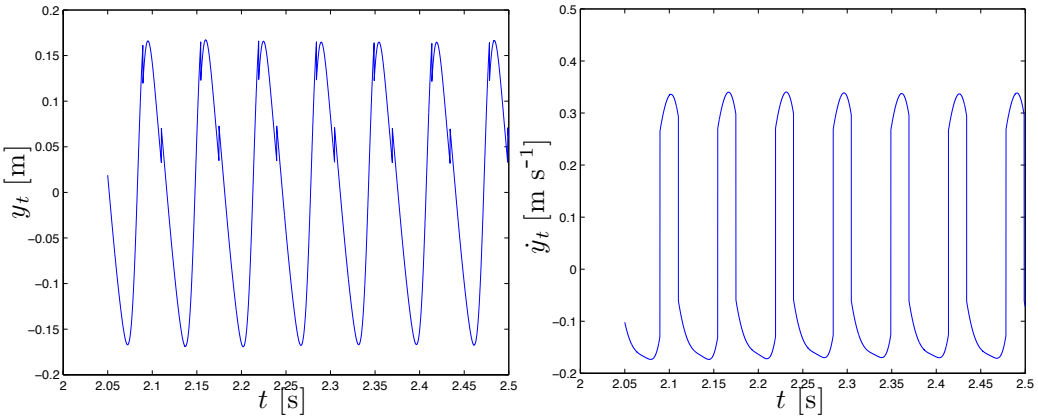

Figure 6: Magnification of graphs y_t and $\dot{y}_t$ around the impact time for $c_1 = c_2 = 2$ mm. There are discontinuities of $\dot{y}_t$.

DSpace VŠB-TUO http://hdl.handle.net/10084/96108 2/4/2013

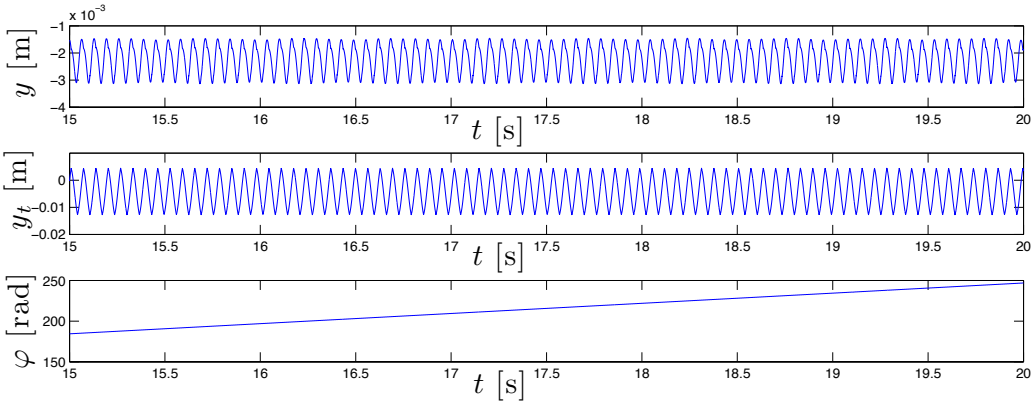

Figure 7: Time responses of the system (17) with parameters given in Table 1 for $c_1 = c_2 = 8$ mm.

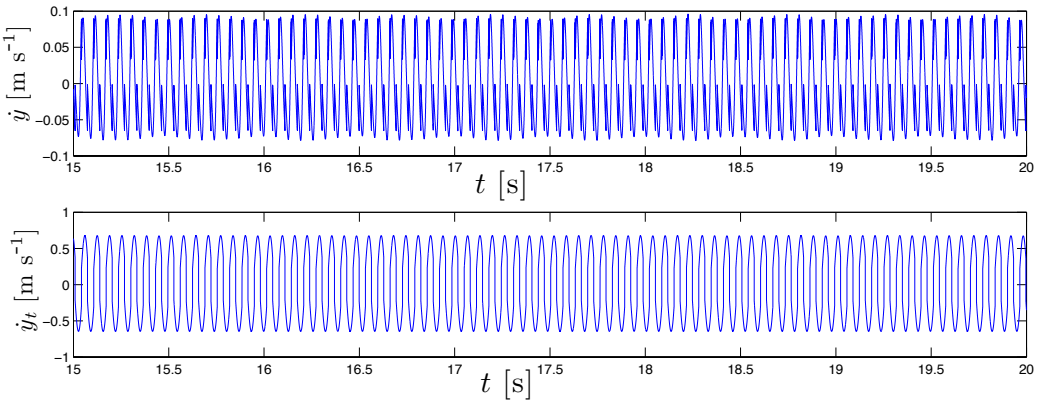

Figure 8: Velocities of an impact element $\dot{y}_t$ and a casing $\dot{y}$ of the system (17) with parameters given in Table 1 for $c_1 = c_2 = 8$ mm.

DSpace VŠB-TUO http://hdl.handle.net/10084/96108 2/4/2013

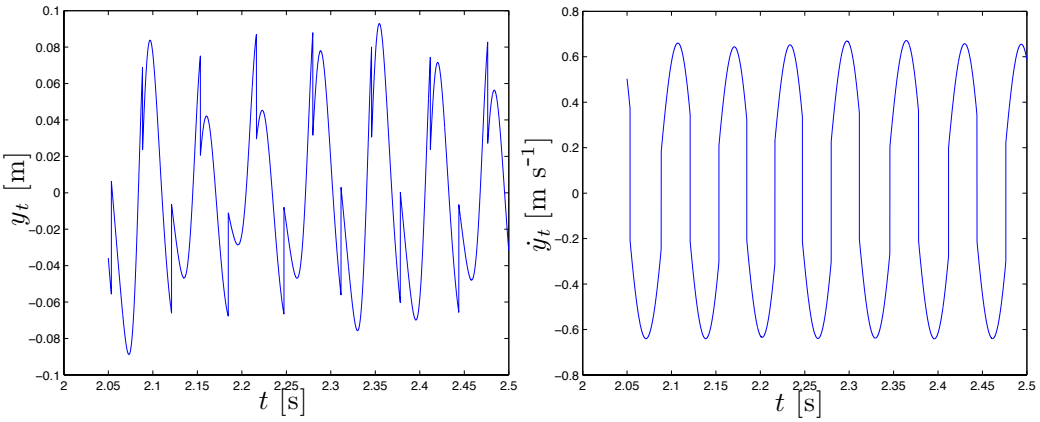

Figure 9: Magnification of graphs y_t and $\dot{y}_t$ around the impact time for $c_1 = c_2 = 8$ mm. There are visible discontinuities of $\dot{y}_t$.

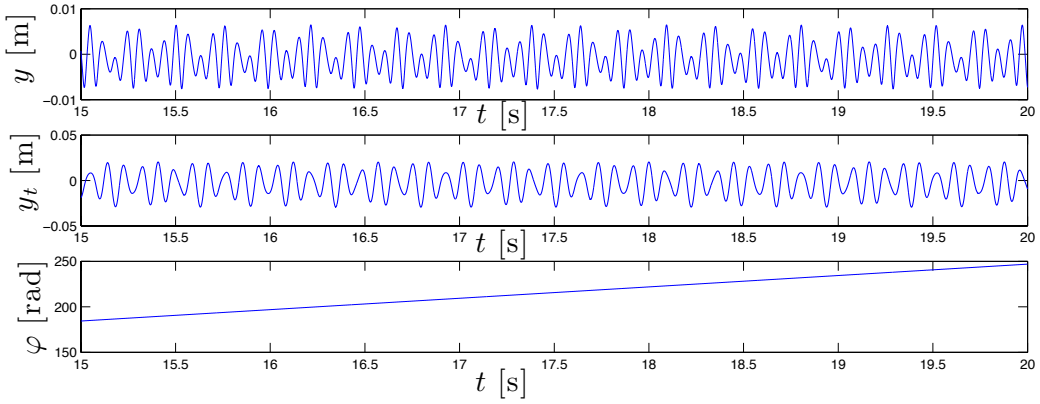

Figure 10: Time responses of the system (17) with parameters given in Table 1 for $c_1 = c_2 = 30$ mm.

DSpace VŠB-TUO http://hdl.handle.net/10084/96108 2/4/2013

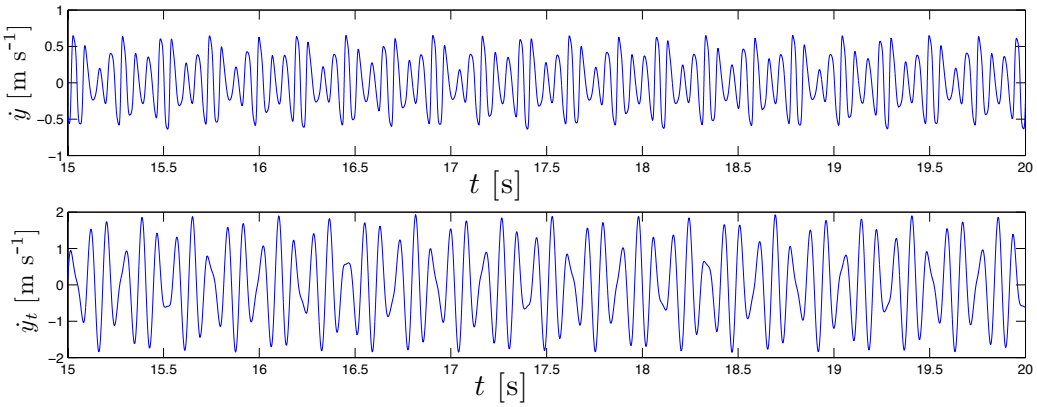

Figure 11: Velocities of an impact element $\dot{y}_t$ and a casing $\dot{y}$ of the system (17) with parameters given in Table 1 for $c_1 = c_2 = 30$ mm.

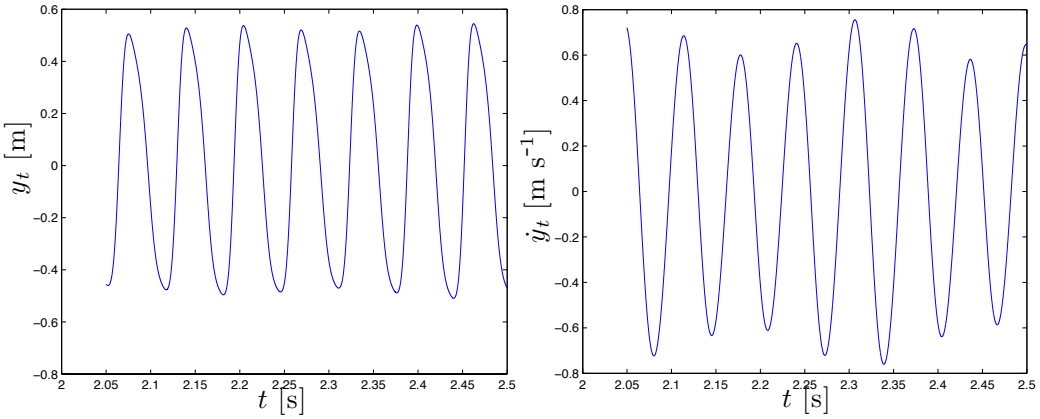

Figure 12: Magnification of graphs y_t and $\dot{y}_t$ for $c_1 = c_2 = 30$ mm. There are no discontinuities of $\dot{y}_t$.

DSpace VŠB-TUO http://hdl.handle.net/10084/96108 2/4/2013

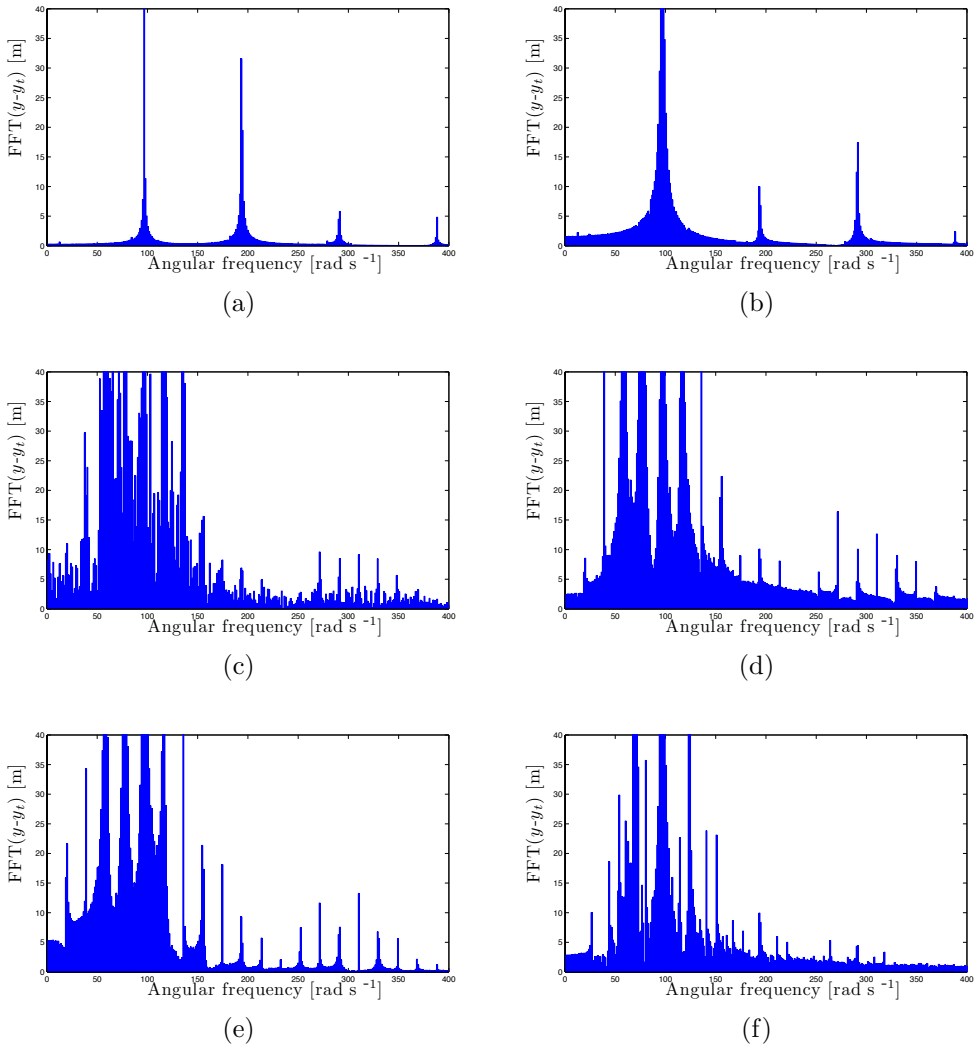

Figure 13: Fourier spectra for parameters given in Table 1 with respect to the change of the upper and lower clearances between the rotor casing and the impact body $c_1 = c_2$: (a) 2 mm, (b) 8 mm, (c) 19 mm, (d) 20 mm, (e) 21 mm and (f) 30 mm.

DSpace VŠB-TUO http://hdl.handle.net/10084/96108 2/4/2013

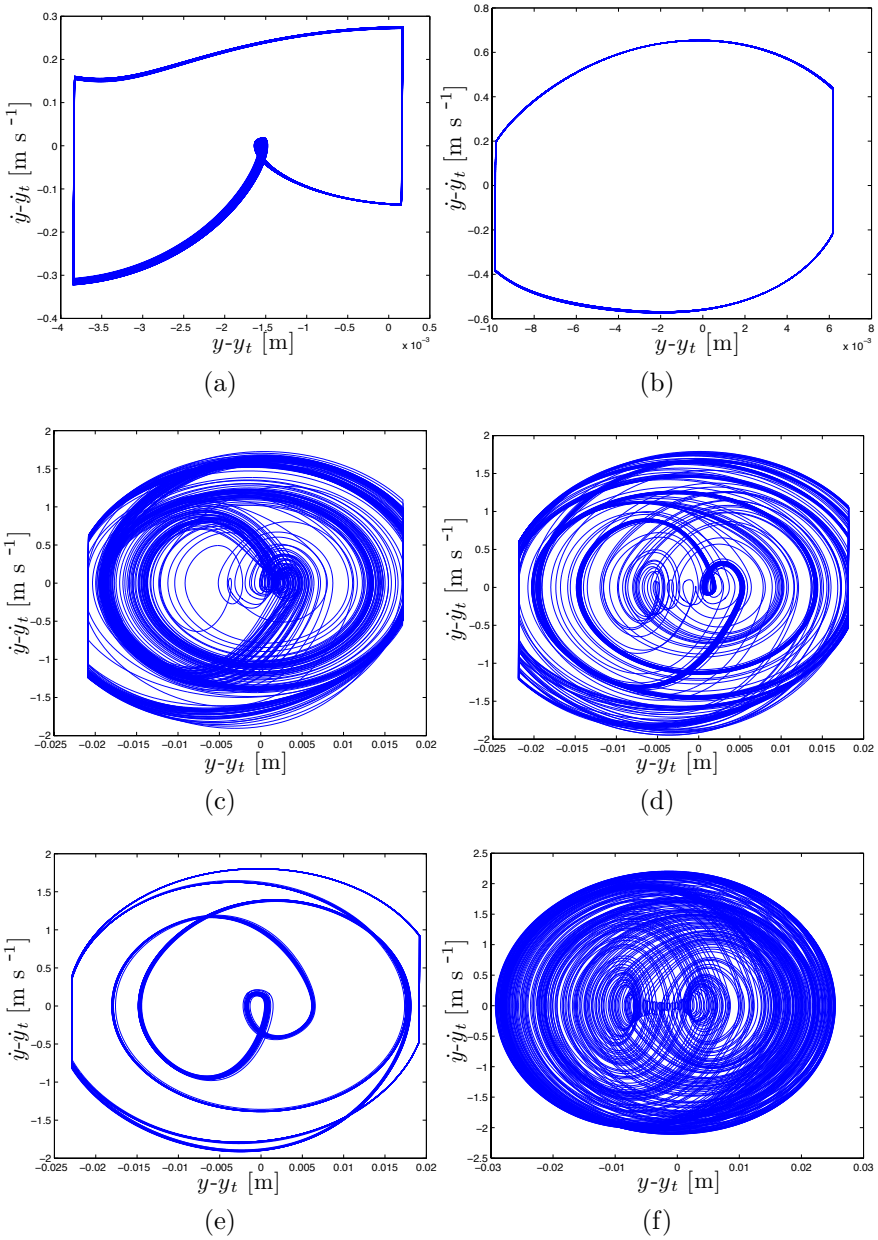

Figure 14: Phase portraits, $y - y_t$ versus $\dot{y} - \dot{y}_t$ for parameters given in Table 1 with respect to the change of the upper and lower clearances between the rotor casing and the impact body $c_1 = c_2$: (a) 2 mm, (b) 8 mm, (c) 19 mm, (d) 20 mm, (e) 21 mm and (f) 30 mm.

DSpace VŠB-TUO http://hdl.handle.net/10084/96108 2/4/2013

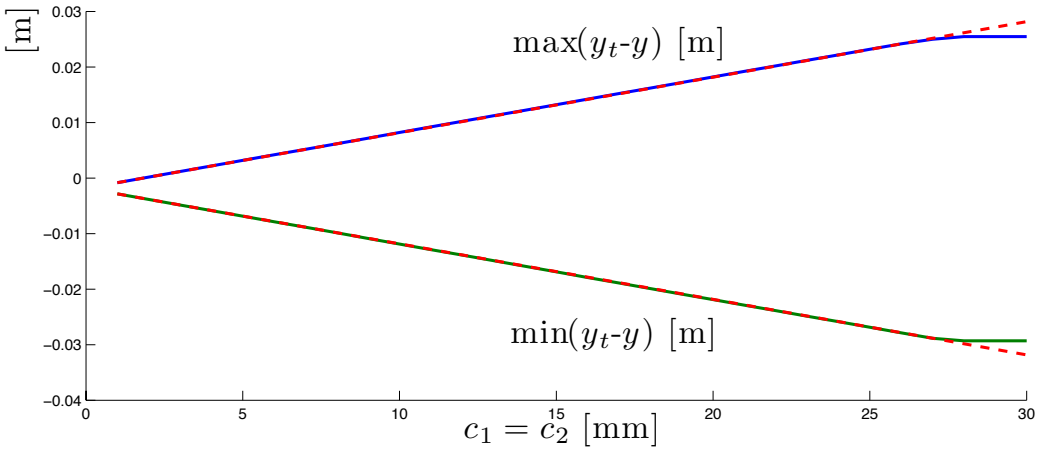

Figure 15: Values of $\max(y_t - y)$ and $\min(y_t - y)$ with respect to $c_1 = c_2$.

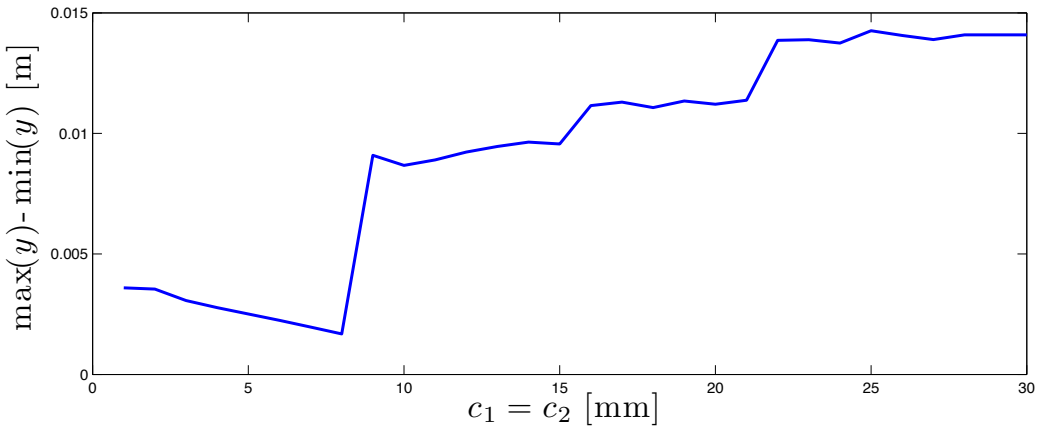

Figure 16: Total vibration amplitude of the rotor frame with respect to $c_1 = c_2$.

DSpace VŠB-TUO http://hdl.handle.net/10084/96108 2/4/2013

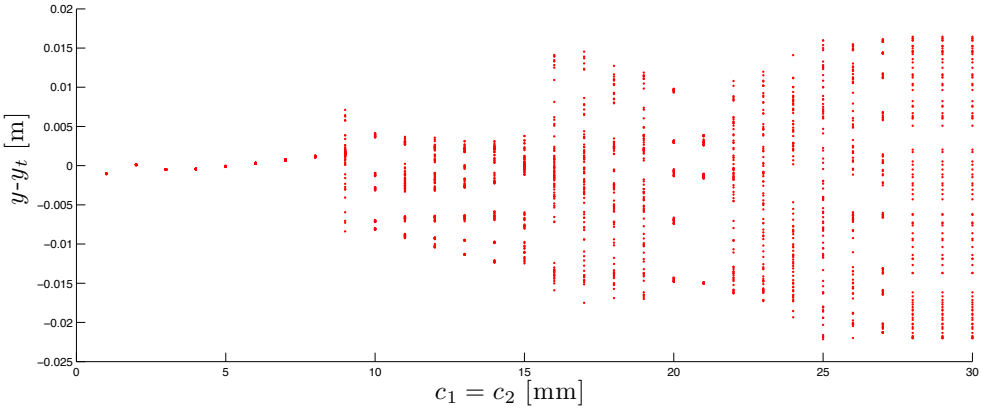

Figure 17: Bifurcation diagram with respect to $c_1 = c_2$.

It was observed that the amplitude of the rotor casing decreases as the clearance increases in the interval from 1 to 8 millimeters. For these clearances the vibration of the rotor casing is close to periodic (or quasiperiodic). If the clearance is equal to 8 mm then the attenuation is significant and the total vibration of the rotor frame is minimal. For clearances greater then 8 mm chaotic behavior is observed, hence clearances less then 8 mm show pre-chaotic movements.

It is also observed that for clearances smaller that 26 millimeters there are double-sided impacts. For clearances greater then 27 mm there are no impacts. The above described bifurcation border was determined by means of computational simulations for the parameters of clearances $c_1 = c_2$.

Acknowledgements

This work was supported by the European Regional Development Fund in the IT4Innovations Centre of Excellence project (CZ.1.05/1.1.00/02.0070).

The work was also supported by the Grant Agency of the Czech Republic, grants No. P101/10/0209, P201/10/0887 and the Ministry of Education of the Czech Republic, project No. MSM6198910027.

References

[1] A.K. Chaterjee, A. Mallik, A. Ghosh, On impact dampers for non-linear vibration systems. Journal of Sound and Vibration **187** (1995) 403–420.

DSpace VŠB-TUO http://hdl.handle.net/10084/96108 2/4/2013

[2] A.K. Chaterjee, A. Mallik, A. Ghosh, Impact dampers for controlling self-excited oscillations Journal of Sound and Vibration **193** (1995) 1003–1014.

[3] J. Warminski, J.M. Balthazar, R.M.L.R.F. Brasil, *Vibrations of a non-ideal parametrically and self-excited model*. Journal of Sound and Vibration **245** (2001) 363–374.

[4] S. L. T. de Souza, I.L. Caldas, J.M. Balthazar, R.M.L.R.F. Brasil, *Analysis of regular and irregular dynamics of a non ideal gear rattling problem*. Journal of Brayilian Society of Mechanical Sciencies, **24** (2002) 111–114.

[5] A.C.J. Luo, D. O' Connor, *Periodic motions with impacting chatter and stick in a gear transmission system*. ASME Journal of Vibration and Acoustics **131** (2009) 041013-1-11

[6] S.L.T. de Souza, I.L. Caldas, R.L. Viana, J.M. Balthazar, R.M.L.R.F. Brasil, *Impact dampers for controlling chaos in systems with limited power supply*. Journal of Sound and Vibration **279** (2005) 955–967.

[7] M. Zukovic, L. Cveticanim, *Chaos in non-ideal mechanical system with clearance*. Journal of Vibration and Control **8** (2009) 1229–1246.

[8] L. Půst, *Electro-mechanical impact system excited by a source of limited power*. Engineering Mechanics **6** (2008) 391–400.

[9] J. Zapoměl, C.H.J. Fox, E. Malenovský, *Numerical investigation of a rotor system with disc-housing impact*. Journal of Sound and Vibration, **243** (2001) 215–240.

DSpace VŠB-TUO http://hdl.handle.net/10084/96108 2/4/2013